Isotopic dependence of superheavy nuclear production in hot fusion reactions

X. J. Bao (包小军),[1] Y. Gao (高远),[2] J. Q. Li (李君清),[1,3] and H. F. Zhang (张鸿飞)[1,*]

[1]*School of Nuclear Science and Technology, Lanzhou University, Lanzhou 730000, People's Republic of China*

[2]*School of Information Engineering, Hangzhou Dianzi University, Hangzhou 310018, People's Republic of China*

[3]*Institute of Modern Physics, Chinese Academy of Science, Lanzhou 730000, People's Republic of China*

(Received 22 August 2015; published 22 September 2015)

The dependence of the evaporation residue cross section (ERCS)'s ability to produce superheavy nuclei (SHN) on the isospin of colliding nuclei is analyzed within the dinuclear system concept. ERCSs are discussed in detail and compared with existing experimental data. The fusion probabilities and surviving probabilities depend sensitively on the neutron numbers of the target and projectile nuclei. In most cases a neutron excess in the system can increase the producing cross section of a new nuclide of SHN. Some predicted ERCSs for the new isotopes of SHN were found to be as large as about 1–8 pb, which is large enough to be realized experimentally with the current existing technology. Element 120 may be produced by ^{50}Ti + ^{251,252}Cf, with the ERCS being about 0.03 pb, and element 119 may be produced by the reaction channel ^{50}Ti + ^{248,249}Bk, with the ERCS being about 0.1 pb via 3*n* and 4*n* emission channels, respectively. Radioactive projectiles are not much more favorable in comparison to stable projectiles.

DOI: 10.1103/PhysRevC.92.034612 PACS number(s): 25.70.Jj, 24.10.Nz, 25.70.Gh, 27.90.+b

I. INTRODUCTION

Since the "island of stability" of superheavy nuclei (SHN) was predicted theoretically, many theoretical models have been explored. With macroscopic-microscopic approaches, a double-magic nucleus was predicted for the ^{298}114 [1–4]. However, the closed shell $Z = 114$ vanishes in the self-consistent models of the mean field with Gogny forces [5] and almost vanishes with all Skyrme forces [6] and in relativistic mean-field models [7–9]. Hartree-Fock calculations with the use of some Skyrme forces predict a double-magic nucleus with $Z = 126$ and $N = 184$ [10]. Relativistic mean-field models and self-consistent mean-field models with Skyrme forces and with Gogny forces predict a closed proton shell for the ^{292}120 nucleus.

The synthesis of SHN in the laboratory has been greatly inspired, and to date all elements up to $Z = 118$ have been synthesized. However, the exact position of the island of stability has not yet been proved in experiments. Experimentally, in cold-fusion reactions, double-closed shell-nuclei of ^{208}Pb or ^{209}Bi are used as targets, while ions heavier than Ar are employed as projectiles. The formed compound nuclei have an excitation energy of about 10–18 MeV. In these cases SHN with $Z = 107$–113 were produced [11–13]. However, from $Z = 107$ to $Z = 113$, the evaporation residue cross section (ERCS) decreases by approximately three orders of magnitude [11]. Furthermore, the formed compound nuclei are neutron deficient. Neutron-rich nuclei have been achieved in the laboratory by ^{48}Ca-induced hot fusion reactions with actinide targets; SHN ($Z = 112$–118) synthesized [14–16] have much larger ERCSs and longer lifetimes compared with those synthesized by cold fusion. In these cases, the excitation energies of compound nuclei are around 30–40 MeV, and the formed compound nucleus can emit three or four neutrons. However, they are still far from the center of the predicted island of stability, and further experimental extension of the region of SHN is limited by available targets, as well as the available reaction mechanism. In recent years, many investigations [17–32] have been devoted to the study of the synthesis mechanism of SHN, however, no approach is currently predominant [33].

To enlarge the scope of the already synthesized SHN, one naturally comes to search for neutron-rich SHN. In the dinuclear system (DNS) conception, the ERCS to produce SHNconsists of three processes: the projectile is caught by the target, and the DNS is formed, which is described by the capture cross section; the DNS evolves from the touching configuration to a compound nucleus in competition with quasifission, which is described by the fusion probability; and the compound nucleus is de-excited by neutron evaporation, which competes with fission (the survival probability). The latter two processes are the most crucial. The survival probability of the formed compound nucleus is expected to increase with increasing neutron number of the composite system, plus the even-odd effect. However, the behavior of the fusion probability is somewhat complicated; it depends on the detailed behavior of the driving potential of the system. To search for the optimal condition of synthesis, it is necessary to study the dependence of the ERCS on the isospin composition of colliding nuclei. One of the aims of the present work is to study several fusion reactions leading to the formation of unknown isotopes of SHN, and those between isotopes already obtained in cold and hot fusion by considering the isospin composition of the colliding nuclei.

Most of the research on this topic has concentrated on predictions of the possible was to synthesize the heaviest elements, $Z = 119$ and 120. Systematic studies of the ERCS of the dependence of the isospin composition of heavy colliding nuclei seem to be rare [34]. In Refs. [30] and [35–39] the isospin-dependent ERCSs for some selected reactions were calculated, although they [35–37] were not compared with

*zhanghongfei@lzu.edu.cn

experimental data. Presently we systematically study the ERCSs of the ^{48}Ca and ^{50}Ti bombarding targets of the actinide isotopic chain.

The paper is organized as follows. In Sec. II, we introduce the general formalism of the DNS model. Numerical results are presented and discussed in Sec. III. First, the ERCSs of SHN with charge numbers $Z = 112$–118 in the xn-evaporation channels are analyzed in detail, then the isotopic dependence of the ERCS is studied within the DNS concept in the reactions leading to SHN. Finally, a brief summary of the results is given in Sec. IV.

II. THEORETICAL FRAMEWORK

In the DNS concept, the ERCS is expressed as [21,40–42]

$$\sigma_{\rm ER}(E_{\rm c.m.}) = \frac{\pi\hbar^2}{2\mu E_{\rm c.m.}} \sum_J (2J+1) T(E_{\rm c.m.}, J) \times P_{\rm CN}(E_{\rm c.m.}, J) W_{\rm sur}(E_{\rm c.m.}, J), \quad (1)$$

where $E_{\rm c.m.}$ is the center-of-mass incident energy and $T(E_{\rm c.m.}, J)$ is the transmission probability of the projectile's overcoming the potential barrier to form a DNS [20,22]. $P_{\rm CN}(E_{\rm c.m.}, J)$ is the probability that the DNS evolves from a touching configuration to a compound nucleus in competition with quasifission. The last term is the survival probability of the formed excited compound nucleus [43]. The sum is over all partial waves J.

The fusion probability is obtained by numerically solving a set of master equations, with the neutron and proton numbers of the projectile-like fragment being variables [44,45]. The distribution probability function, $P(Z_1, N_1, E_1, t)$, at time t to find Z_1 protons and N_1 neutrons in fragment 1 with excitation energy E_1, obeys the following master equation:

$$\begin{aligned}\frac{dP(Z_1,N_1,E_1,t)}{dt} &= \sum_{Z_1'} W_{Z_1,N_1;Z_1',N_1}(t)[d_{Z_1,N_1}P(Z_1',N_1,E_1',t) \\ &- d_{Z_1',N_1}P(Z_1,N_1,E_1,t)] + \sum_{N_1'} W_{Z_1,N_1;Z_1,N_1'}(t) \\ &\times [d_{Z_1,N_1}P(Z_1,N_1',E_1',t) - d_{Z_1,N_1'}P(Z_1,N_1,E_1,t)] \\ &- [\Lambda_{qf}(\Theta(t)) + \Lambda_{fs}(\Theta(t))]P(Z_1,N_1,E_1,t), \end{aligned} \quad (2)$$

where $W_{N_1,Z_1;N_1',Z_1}$ is the mean transition probability from channel (N_1', Z_1, E_1') to channel (N_1, Z_1, E_1), while d_{N_1,Z_1} denotes the microscopic dimension corresponding to macroscopic state (N_1, Z_1, E_1). The sum is taken over all possible proton and neutron numbers that fragments Z_1' and N_1' may take, but only one nucleon transfer is considered in the model with $Z_1' = Z_1 \pm 1$ and $N_1' = N_1 \pm 1$. The excitation energy E_1 is determined by the dissipation energy from the relative motion [46,47] and the potential energy surface (PES) of the DNS. The motion of nucleons in the interacting potential is governed by the single-particle Hamiltonian and the interaction. The evolution of the DNS along the distance between nuclei R leads to quasifission. The quasifission rate $\Lambda_{\rm qf}$ and fission rate (for a heavy fragment) $\Lambda_{\rm fs}$ are estimated with the one-dimensional Kramers formula [48,49].

In the relaxation process of the relative motion, nuclei are excited by the dissipation of the relative kinetic energy. The local excitation energy is determined by this transferred excitation energy of the composite system and the PES of the DNS. The PES is given by

$$\begin{aligned} U(N_1,Z_1,N_2,Z_2,R,\beta_1,\beta_2,J) &= B(N_1,Z_1,\beta_1) + B(N_2,Z_2,\beta_2) \\ &- [B(N,Z,\beta) + V_{\rm rot}^{\rm CN}(J)] + U_C(Z_1,Z_2,\beta_1,\beta_2,R) \\ &+ U_N(N_1,Z_1,N_2,Z_2,R,\beta_1,\beta_2,J), \end{aligned} \quad (3)$$

where $N = N_1 + N_2$ and $Z = Z_1 + Z_2$. $\beta_i (i = 1,2)$ and β represent the quadrupole deformation of the two fragments and compound nucleus, respectively. R is the distance between nuclei at which the interaction potential between the two nuclei $U_C + U_N$ has the minimum value. $B(N_1, Z_1, \beta_1)$, $B(N_2, Z_2, \beta_2)$, and $B(N, Z, \beta)$ are the binding energies of the two deformed nuclei and compound nucleus, respectively. $U_C(Z_1, Z_2, \beta_1, \beta_2, R)$, $U_N(N_1, Z_1, N_2, Z_2, R, \beta_1, \beta_2, J)$, and $V_{\rm rot}^{\rm CN}(J)$ are the Coulomb, nuclear interaction potential, and centrifugal energy, respectively. The Coulomb interaction can be calculated with Wong's formula [50], and the nuclear potential is calculated with a Skyrme-type interaction without considering the momentum and spin dependence (see Ref. [51] and references therein).

Figures 1(a) and 1(b) show the driving potential for the reaction systems ^{48}Ca + ^{242}Pu and ^{50}Ti + ^{242}Pu as functions of N_1 and Z_1, respectively. The incident channel is shown by the white circle, and the thick central (red) line indicates the valley of the PES. It turns out that there is a valley in the two-variable (N_1, Z_1) driving potential, and for the ^{48}Ca-induced reaction ^{48}Ca + ^{242}Pu, the injection point is located in the valley. In Fig. 1(b) the incident channel is not in the valley, but at a place higher than that. Thus the distribution probability starts at the injection point, reaches the valley, and then, in the valley, flows both in the symmetrical direction and in the direction of the compound nuclear formation. Obviously the one-variable (A_1) master equation cannot correctly describe the ^{50}Ti + ^{242}Pu reaction process.

The compound nucleus formation probability at the Coulomb barrier B, corresponding to a certain orientation of the colliding nuclei in the entrance channel, and for the angular momentum J is given by

$$P_{\rm CN}(E_{\rm c.m.}, J, B) = \sum_{Z_1=1}^{Z_{\rm BG}} \sum_{N_1=1}^{N_{\rm BG}} P(Z_1, N_1, E_1, \tau_{\rm int}). \quad (4)$$

The interaction time $\tau_{\rm int}$ in the dissipative process of two colliding nuclei is dependent on the incident energy $E_{\rm c.m.}$, J, and B, which are determined using the deflection function method [27]. We obtain the fusion probability as

$$P_{\rm CN}(E_{\rm c.m.}, J) = \int f(B) P_{\rm CN}(E_{\rm c.m.}, J, B)\, {\rm dB}. \quad (5)$$

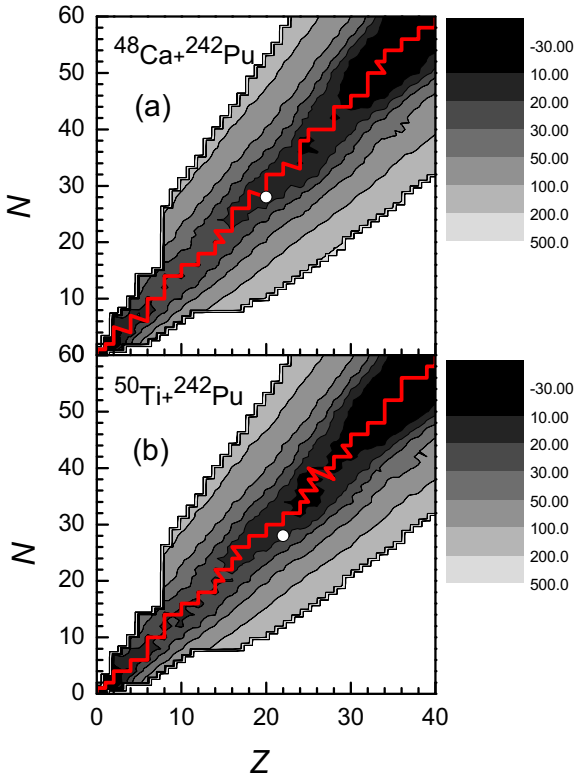

FIG. 1. (Color online) Contour plot of the driving potential for the reaction systems (a) ^{48}Ca + ^{242}Pu and (b) ^{50}Ti + ^{242}Pu as functions of the neutron and proton numbers of fragment 1. Incident channels are indicated. Thick central (red) lines indicate the valley of the potential.

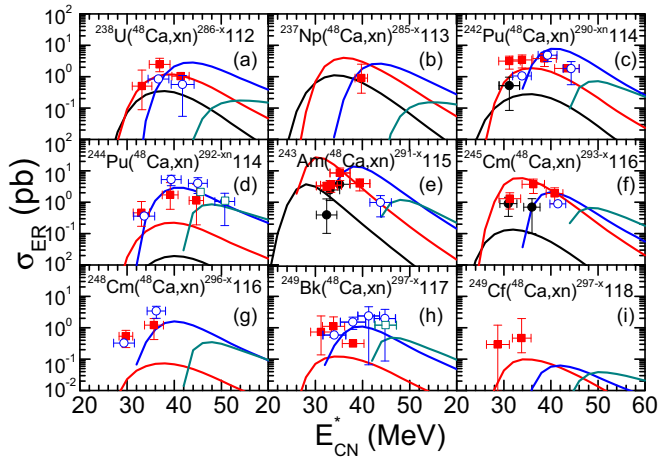

FIG. 2. (Color online) Calculated ERCSs compared with available experimental data for the reactions ^{48}Ca + ^{238}U [52], ^{48}Ca + ^{237}Np [53], ^{48}Ca + ^{242}Pu [52], ^{48}Ca + ^{244}Pu [55], ^{48}Ca + ^{243}Am [54], ^{48}Ca + ^{245}Cm [56], ^{48}Ca + ^{248}Cm [52], ^{48}Ca + ^{249}Bk [57], and ^{48}Ca + ^{249}Cf [56]. Measured ERCSs of the 2n, 3n, 4n, and 5n channels are denoted by filled black circles, filled (red) squares, open (blue) circles, and open (dark cyan) squares, respectively. Calculated results are denoted by solid lines.

III. NUMERICAL RESULTS AND DISCUSSION

A. Production cross sections of isotopes with $Z = 112$–118 in ^{48}Ca-induced reactions

It is found from data that there are not many differences in magnitude among the ERCSs regarding the production of elements $Z = 112$–118, and they are all at the picobarn level. This phenomenon is thought to be due to the increasing fission barriers, which owe to the larger shell corrections, and that these synthesized elements are approaching the neutron and proton closed shells in the region of the island of stability [32,58,59]. Systematic calculations have been made to describe the ERCSs in ^{48}Ca-induced hot fusion reactions with the Langevin dynamics model [60–62], the fusion-by-diffusion model [29], the DNS model [27,28,32], and a phenomenological version of the DNS model [25]. All these theories can reasonably reproduce the data, however, a simple agreement between theoretical results and experimental data is not sufficient to reveal the essential substances of the phenomena involved. Actually, the fact is that all the above theories have provided approximately the same product $W_{\rm sur}P_{\rm CN}$. The theory to evaluate the survival probability $W_{\rm sur}$ is better established, but some parameters used in it have not been well estimated to date. To understand the fusion probability $P_{\rm CN}$ is very important, even for correctly choosing the correct parameter set for $W_{\rm sur}$. Though all the above theories can reasonably reproduce the data we are aware that the calculated $P_{\rm CN}$ values differ significantly one from another. These different results evaluated with different models may reflect the fact that there is still large uncertainty in the prediction of the ERCS of SHN. Presently (see Fig. 2), based on the DNS, the excitation functions for different xn channels for the hot fusion channels ^{238}U(^{48}Ca,xn)$^{286-x}$112, ^{237}Np(^{48}Ca,xn)$^{285-x}$113, ^{242}Pu(^{48}Ca,xn)$^{290-x}$114, ^{244}Pu(^{48}Ca,xn)$^{292-x}$114, ^{243}Am(^{48}Ca,xn)$^{291-x}$115, ^{245}Cm(^{48}Ca,xn)$^{293-x}$116, ^{248}Cm(^{48}Ca,xn)$^{296-x}$116, ^{249}Bk(^{48}Ca,xn)$^{297-x}$117, and ^{249}Cf(^{48}Ca,xn)$^{297-x}$118 for producing elements $Z = 112$–118 were systematically studied, and the corresponding experimental data [52–57] are indicated for comparison, where the displayed error bars correspond to the statistical uncertainties only. Taking into account the experimental uncertainties one can say that the agreement between our calculated ERCSs and the experimental values is good for most of the evaporation channels, especially for 3n and 4n emission. Careful observation shows that for the ^{237}Np(^{48}Ca,xn)$^{285-x}$113, ^{243}Am(^{48}Ca,xn)$^{291-x}$115, ^{245}Cm(^{48}Ca,xn)$^{293-x}$116, and ^{249}Cf(^{48}Ca,xn)$^{297-x}$118 channels, the maximal $\sigma_{\rm ER}$ is found in the 3n emission channel, and for the ^{242}Pu(^{48}Ca,xn)$^{290-x}$114, ^{244}Pu(^{48}Ca,xn)$^{292-x}$114, ^{248}Cm(^{48}Ca,xn)$^{296-x}$116, and ^{249}Bk(^{48}Ca,xn)$^{297-x}$117 channels, the maximal $\sigma_{\rm ER}$ is found in the 4n channel. These results are well in coincidence with the experimental data [52–57]. Whether the maximal $\sigma_{\rm ER}$ appears in the 3n or in 4n channel is decided by the behavior of $W_{\rm sur}$ and $P_{\rm cn}$ with increasing excitation energy. The fusion probability increases with increasing excitation energy, while the survival probability for each neutron emission channel increases with increasing excitation energy up to a maximum value, and then decreases with the excitation energy. Usually the maximal

$W_{\rm sur}^{3n}$ is larger than the maximal $W_{\rm sur}^{4n}$. Therefore, whether the maximal ERCS appears in the $3n$ or in the $4n$ channel depends on the increasing behavior of $P_{\rm cn}$ with the excitation energy. In terms of an angular-momentum-dependent version of the fusion-by-diffusion model [29] with fission barriers and ground-state masses taken from the Warsaw macroscopic-microscopic model [63,64], Siwek-Wilczynska *et al.* have studied the ERCS of SHN $Z = 114$–118. For ^{244}Pu(^{48}Ca,xn)$^{292-x}$114 and ^{248}Cm(^{48}Ca,xn)$^{296-x}$116, they concluded that the ERCS for the $3n$ channel is a bit larger than that for the $4n$ channel. However, the maximal $\sigma_{\rm ER}$ is found for the $4n$ channel in the experiment. Zagrebaev *et al.* have systematically studied the ERCSs for $Z = 112$–118, and they found that the result for all reactions in the $3n$ channel is a bit larger than that for the $4n$ channel [58,59]. This is probably because the fusion probability remains almost constant at the level of 10^{-3} for $Z = 114$–118 at excitation energies $E^* \geqslant 30$ MeV. Recently, Zagrebaev *et al.* further calculated the ERCSs for these hot fusion systems [62]; they found that the experimental data were reproduced except for the channel ^{242}Pu(^{48}Ca,xn)$^{290-x}$114. The correct product $W_{\rm sur}P_{\rm CN}$ may give the correct ERCS, however, it cannot correctly describe the fusion-evaporation process. It turns out that the fusion probability and thus the fusion-evaporation process for SHN production can be reasonably described by the current model.

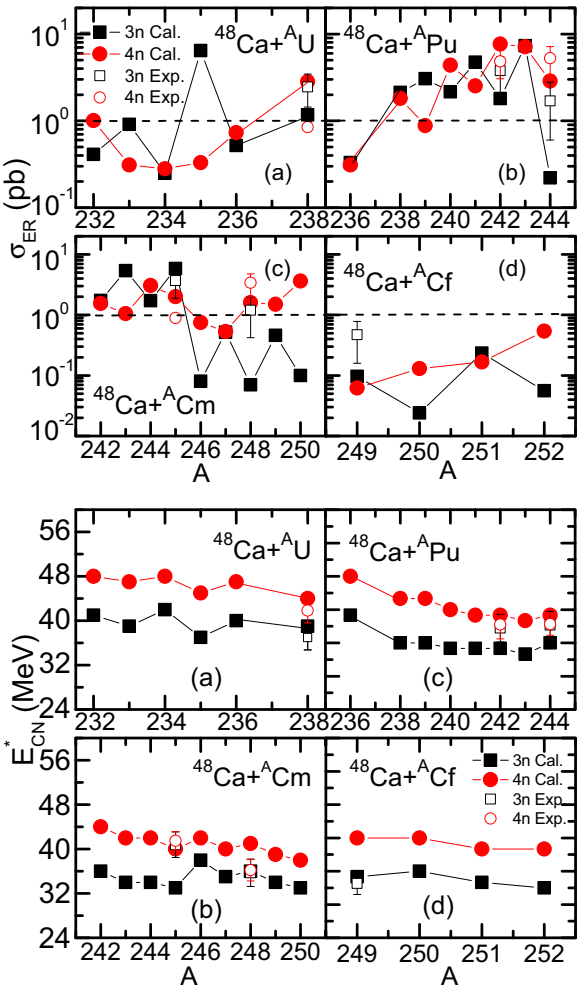

FIG. 3. (Color online) Top: Isospin dependence of the maximal evaporation residue cross sections from the hot fusion reactions (a) ^{48}Ca+^{A}U, (b) ^{48}Ca+^{A}Pu, (c) ^{48}Ca+^{A}Cm, and (d) ^{48}Ca+^{A}Cf as functions of the target mass number A, for the $3n$ and $4n$ emission channels. The corresponding experimental data are represented by the open squares ($3n$) and open circles ($4n$) with error bars. Bottom: Corresponding excitation energies of the compound nuclei.

B. Isospin dependence of the ERCSs of SHN

In order to study the possibility of synthesizing more neutron-rich SHN, or new SHN, we study the isospin dependence of the ERCSs of SHN. ^{48}Ca is used to bombard some actinium isotopic chains. It is known that the ERCS of SHN mainly depends on the fusion probability $P_{\rm CN}$ and survival probability $W_{\rm sur}$. The heavy-ion fusion process is not yet fully understood; it depends on the details of the driving potential. Not only is the numerical value of the fusion probability $P_{\rm CN}$ uncertain, but the dependence of $P_{\rm CN}$ on the excitation energy and the reaction entrance channel is not well established. Furthermore, the survival probability depends on

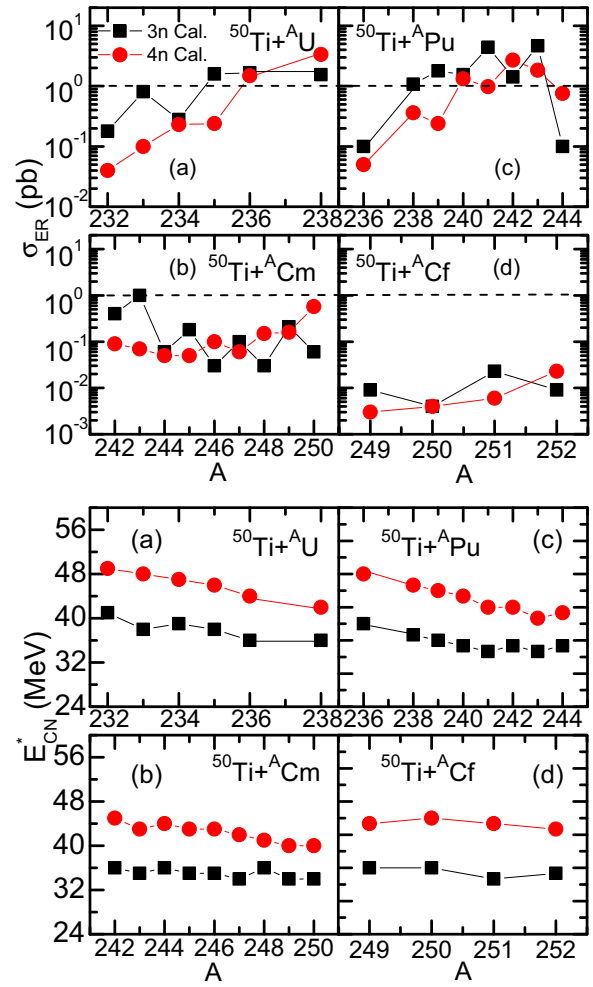

FIG. 4. (Color online) The same as Fig. 3, but for ^{50}Ti-induced hot fusion reactions.

the fission barrier, neutron separation energy, level density parameter, ratio a_f/a_n, shell damping factor, and so on. Our studies for all investigations were performed with one set of parameters and with the same assumptions. In Fig. 3 (top) the maximal ERCS, σ_{ER}(pb), for $3n$ and $4n$ emission channels of ^{48}Ca-bombarding actinium isotopic chains U, Pu, Cm, and Cf are shown as a function of the mass number of the target, with corresponding experimental data indicated for comparison. The corresponding excitation energies to emit three and four neutrons are shown in Fig. 3 (bottom). Except in the $3n$ emission channel for the $^{48}\mathrm{Ca} + {}^{A}\mathrm{Cm}$ channel, in all channels it is shown that the ERCSs basically increase with increasing neutron number, though sometimes not very distinctly.

Generally, the survival probability increases with increasing neutron number of the compound nucleus in addition to the even-odd effect and decreases with the excitation energy. The behavior of the fusion probability P_{CN} changes with increasing neutron number of the targets and is not regular; it depends on the details of the driving potential, which is decided by the properties of the nuclei in each DNS and their interactions. And P_{CN} decreases with decreasing excitation energy. Figure 3 (bottom) shows that the excitation energies to emit three and four neutrons slowly decrease with increasing neutron number. This means that roughly with increasing neutron number W_{sur} should increase and P_{CN} should decrease. We are aware that during the calculation the fusion probability P_{CN} for $^{48}\mathrm{Ca} + {}^{A}\mathrm{U}$, $^{48}\mathrm{Ca} + {}^{A}\mathrm{Cm}$, and $^{48}\mathrm{Ca} + {}^{A}\mathrm{Cf}$ decreases with increasing neutron; for $^{48}\mathrm{Ca} + {}^{A}\mathrm{Pu}$ the P_{CN} changes with increasing neutron number of the target and is not regular. However, in most cases, the increases in W_{sur} are not canceled by the decreasing P_{CN} with increasing neutron number. Therefore, there are certain probabilities of producing new nuclides such as using ^{48}Ca to bombard ^{232,233,235,236}U, $^{238-244}$Pu, $^{242-250}$Cm, and ^{250,251,252}Cf. Figure 4 shows the same thing as Fig. 3. It can be seen that some new nuclides of $Z = 114$, 116, and 118 could be produced by the reactions $^{50}\mathrm{Ti} + {}^{233,235,236,238}$U, $^{50}\mathrm{Ti} + {}^{238-244}$Pu, and $^{50}\mathrm{Ti} + {}^{242,243,249,250}$Cm. Hopefully, this can shed some light on new SHN production.

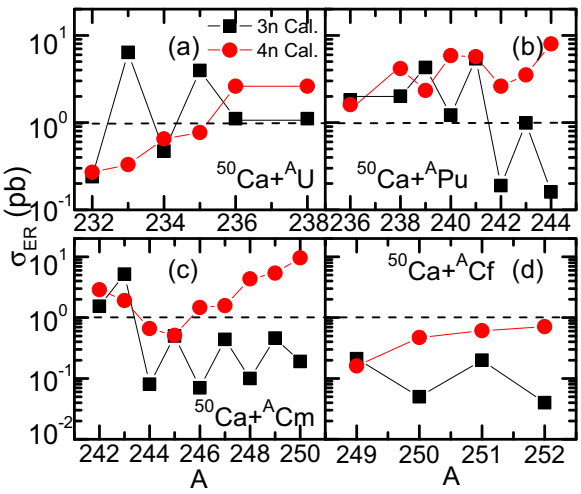

FIG. 5. (Color online) The same as Fig. 3, but for ^{50}Ca-induced hot fusion reactions.

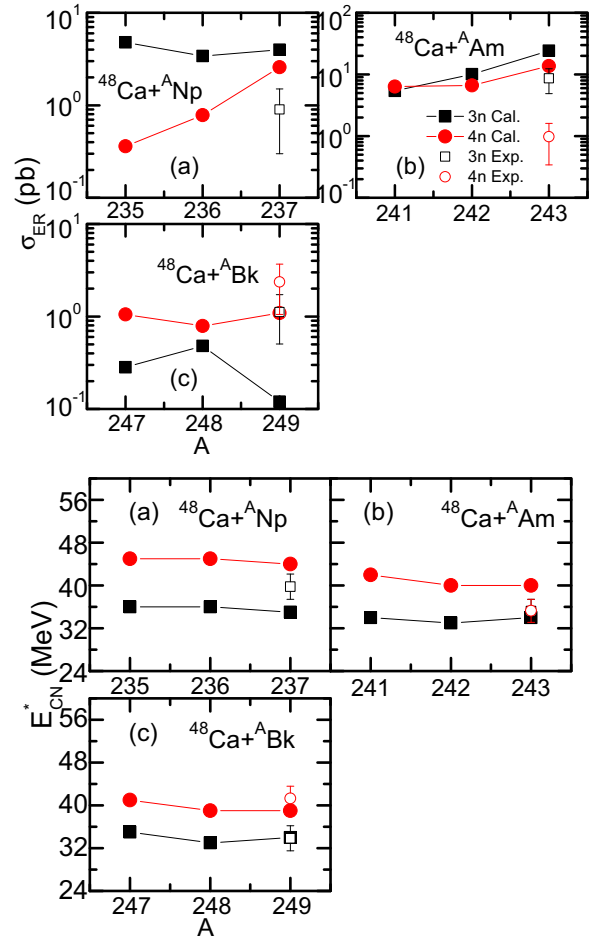

FIG. 6. (Color online) The same as Fig. 3, but for $^{48}\mathrm{Ca} + {}^{A}$Np, $^{48}\mathrm{Ca} + {}^{A}$Am, and $^{48}\mathrm{Ca} + {}^{A}$Bk.

Radioactive beams may likely be produced with high intensities in the near-future. In actinide-based reactions the use of neutron-rich projectiles of ^{50}Ca (Fig. 5) leads to superheavy nucleus production, it is found that the obtained ERCSs for corresponding SHN are comparable with those obtained using ^{48}Ca (Fig. 3). However, the intensities of radioactive beam ^{50}Ca are significantly lower, by three orders of magnitude, than those of the stable beam ^{48}Ca. Therefore, using stable beam ^{48}Ca is predicted to be a favorable method for producing SHNs located between those produced by cold and hot fusion reactions.

Moreover, it is shown in Figs. 3 and 4 that in most cases the ERCSs for $Z = 114$ and 116 are larger than those for $Z = 112$. This is due to the strong influence of the $Z = 114$ and $N = 184$ shell [3,37]. With the ^{48}Ca and the ^{50}Ti beams the production of SHN with odd Z is investigated as well. From our calculated results, shown in Figs. 6 and 7, one can expect large ERCSs in actinide-based reactions with the ^{48}Ca beam. And based on the targets ^{236}Np, ^{242}Am, and ^{248}Bk the production of odd SHN, with $Z = 113$, 115, and 117, is shown optimistically. Similar results can be observed with ^{50}Ti projectiles. The reactions $^{50}\mathrm{Ti} + {}^{236}$Np, $^{50}\mathrm{Ti} + {}^{242}$Am, and $^{50}\mathrm{Ti} + {}^{248}$Bk are most favorable for the production of odd SHN with charge numbers 115, 117, and 119, respectively.

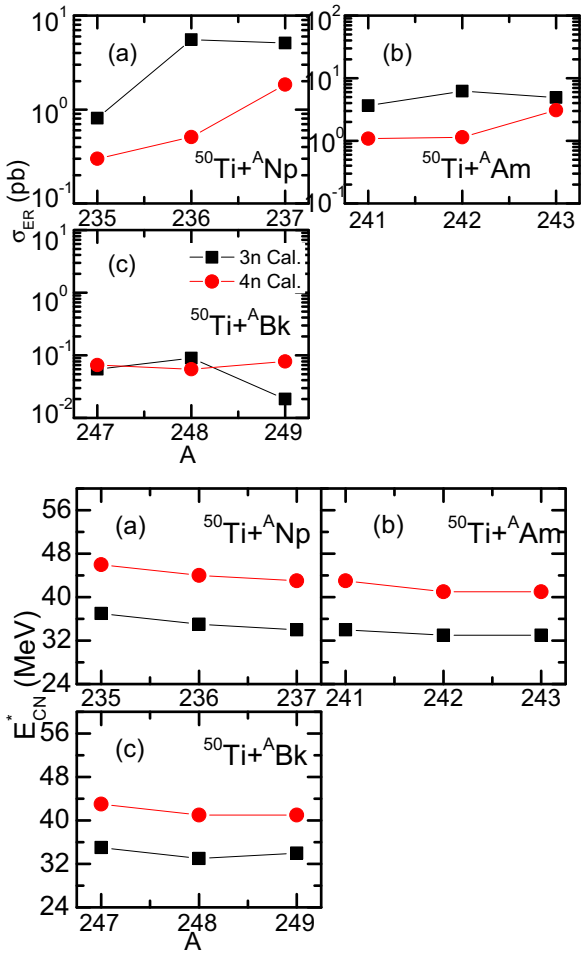

FIG. 7. (Color online) The same as Fig. 6, but for ^{50}Ti-induced hot fusion reactions.

C. ^{248}Cm-based reactions

Calculated maximal ERCSs are plotted in Fig. 8 using the ^{248}Cm target. The ERCSs decrease by about five orders of magnitude with increasing charge number of the projectile from $Z = 18$ to $Z = 24$. This is due to the strong decrease in the fusion probability P_{CN} and the increase in the quasifission with increasing charge number of the compound nucleus. At a fixed charge asymmetry in the entrance channel, the fusion probability P_{CN} of the compound nucleus decreases with increasing neutron excess in the projectile. In Fig. 8, except for the projectiles ^{48}Ca, ^{50}Ti, and ^{54}Cr, which are stable nuclei, all others are radioactive nuclei. And from Fig. 8 one can conclude that the radioactive isotopes of the projectile nucleus with the largest neutron excess are unfavorable for most cases of hot fusion. In ^{248}Cm-based reactions the use of neutron-rich projectiles leads to ERCSs which are comparable with those from stable projectiles. If the intensity of the radioactive beams is lower than the intensity of the stable nuclear beam, then the time of illumination with a radioactive beam must be long enough to achieve the same cross section. In most cases the intensities of the radioactive beams are significantly lower than those of the stable beams; stable beams are preferred rather than using radioactive beams for SHN production.

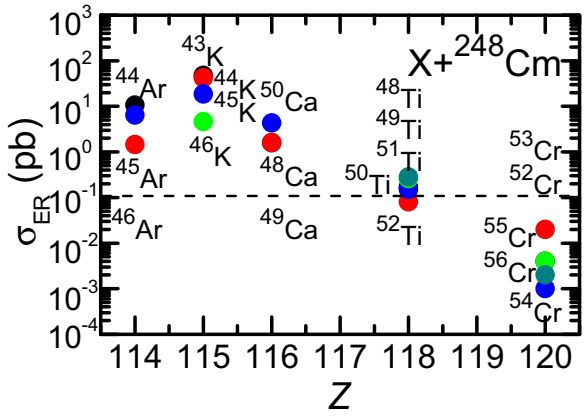

FIG. 8. (Color online) Calculated maximal ERCSs for ^{248}Cm-based hot fusion reactions. According to the increasing mass number of the projectile, results are shown by black, red, blue, green, and dark cyan circles.

IV. SUMMARY

To shed light on the conditions for synthesizing some new superheavy elements and new superheavy nuclides, the projectiles ^{48}Ca, ^{50}Ti, and ^{50}Ca bombarding some actinide isotope chains are systematically studied within the DNS model; therefore the isospin effect on the ERCS is demonstrated. The ERCS is mainly dependent on the fusion and survival probabilities of the compound nucleus. The survival probability increases with increasing neutron number of the target in addition to the even-odd effect. However, the fusion probability changes with the neutron number of the target irregularly, depending on the details of the driving potential, and should be studied individually. For the reactions in Fig. 3, for most cases, the increases in W_{sur} are not canceled by the decreasing P_{CN} with increasing neutron. Therefore, there are certain probabilities to produce new nuclides such as using ^{48}Ca to bombard ^{232,233,235,236}U, $^{238-244}$Pu, $^{242-250}$Cm, and ^{250,251,252}Cf. Then one can expect to produce new superheavy nuclides of elements 112, 114, and 116 with ERCSs larger than from about 1 up to 8 pb. For the reactions in Fig. 4, it can be seen that some new nuclides of elements 114, 116, and 118 may be produced by the reactions $^{50}\text{Ti} + {}^{233,235,236,238}\text{U}$, $^{50}\text{Ti} + {}^{238-244}\text{Pu}$, and $^{50}\text{Ti} + {}^{243,250}\text{Cm}$, with ERCSs from about 1 to 4 pb. And element 120 may be produced by $^{50}\text{Ti} + {}^{251,252}\text{Cf}$, with the ERCS being about 0.03 pb. Some new nuclides of elements 113, 115, and 117 may be produced by the reaction channels $^{48}\text{Ca} + {}^{236}\text{Np}$, $^{48}\text{Ca} + {}^{242}\text{Am}$, and $^{48}\text{Ca} + {}^{248}\text{Bk}$, with the ERCSs larger than 1 pb. Some new nuclides of elements 115 and 117 may be produced by the reaction channels $^{50}\text{Ti} + {}^{236}\text{Np}$ and $^{50}\text{Ti} + {}^{242}\text{Am}$, with the ERCS larger than 1 pb. And element 119 may be produced by the reaction channel $^{50}\text{Ti} + {}^{248,249}\text{Bk}$, with the ERCS being about 0.1 pb via $3n$ and $4n$ channels, respectively. Radioactive projectiles are not much more favorable in comparison to stable projectiles. Hopefully, the results will shed light on the experimentaly synthesis of some new nuclides and new elements.

ACKNOWLEDGMENTS

J.Q.L. is grateful for the discussions with Jieding Zhu. The work was supported by the National Natural Science Foundation of China (Grant Nos. 11175074, 11475050, 11120101005, and 11265013), Fundamental Research Funds for the Central Universities (Grantlzujbky-2014-230), and CAS Knowledge Innovation Project No. KJCX2-EW-N01.

[1] U. Mosel and W. Greiner, Z. Phys. **222**, 261 (1969).
[2] S. G. Nilsson, C. F. Tsang, A. Sobiczewski, Z. Szymanski, S. Wycech, C. Gustafson, I.-L. Lamm, P. Möller, and B. Nilsson, Nucl. Phys. A **131**, 1 (1969).
[3] P. Möller *et al.*, At. Data Nucl. Data Tables **59**, 185 (1995).
[4] R. Smolańczuk, Phys. Rev. C **56**, 812 (1997).
[5] J. Decharge, J. F. Berger, K. Dietrich, and M. S. Weiss, Phys. Lett. B **451**, 275 (1999).
[6] M. Bender, W. Nazarewicz, and P. G. Reinhard, Phys. Lett. B **515**, 42 (2001).
[7] P. Ring, Prog. Part. Nucl. Phys. **37**, 193 (1996).
[8] J. Meng, H. Toki, S. G. Zhou, S. Q. Zhang, W. H. Long, and L. S. Geng, Prog. Part. Nucl. Phys. **57**, 470 (2006).
[9] J. J. Li, W. H. Long, J. Margueron, and N. Van Giai, Phys. Lett. B **732**, 169 (2014).
[10] S. Cwiok, J. Dobaczewski, P. H. Heenen, P. Magierski, and W. Nazarewicz, Nucl. Phys. A **611**, 211 (1996).
[11] S. Hofmann and G. Münzenberg, Rev. Mod. Phys. **72**, 733 (2000).
[12] S. Hofmann, Radiochim. Acta **99**, 405 (2011).
[13] K. Morita *et al.*, J. Phys. Soc. Jpn. **76**, 045001 (2007).
[14] Y. T. Oganessian, J. Phys. G: Nucl. Part. Phys. **34**, R165 (2007).
[15] Y. T. Oganessian *et al.*, Phys. Rev. Lett. **104**, 142502 (2010).
[16] Y. T. Oganessian, Radiochim. Acta **99**, 429 (2011).
[17] W. J. Swiatecki, Prog. Part. Nucl. Phys. **4**, 383 (1980).
[18] Y. Aritomo, T. Wada, M. Ohta, and Y. Abe, Phys. Rev. C **59**, 796 (1999).
[19] C. W. Shen, Y. Abe, D. Boilley, G. Kosenko, and E. G. Zhao, Int. J. Mod. Phys. E **17**, 66 (2008).
[20] V. I. Zagrebaev, Phys. Rev. C **64**, 034606 (2001).
[21] G. G. Adamian *et al.*, Nucl. Phys. A **627**, 361 (1997); **633**, 409 (1998).
[22] Z. Q. Feng, G. M. Jin, F. Fu, and J. Q. Li, Nucl. Phys. A **771**, 50 (2006).
[23] V. Zagrebaev and W. Greiner, Phys. Rev. C **78**, 034610 (2008).
[24] R. Smolańczuk, Phys. Rev. C **81**, 067602 (2010).
[25] N. Wang, J. Tian, and W. Scheid, Phys. Rev. C **84**, 061601(R) (2011).
[26] L. Zhu, W. J. Xie, and F.-S. Zhang, Phys. Rev. C **89**, 024615 (2014).
[27] Z. Q. Feng, G. M. Jin, J. Q. Li, and W. Scheid, Phys. Rev. C **76**, 044606 (2007).
[28] N. Wang, E. G. Zhao, W. Scheid, and S. G. Zhou, Phys. Rev. C **85**, 041601(R) (2012).
[29] K. Siwek-Wilczyńska, T. Cap, M. Kowal, A. Sobiczewski, and J. Wilczyński, Phys. Rev. C **86**, 014611 (2012).
[30] G. Mandaglio, G. Giardina, A. K. Nasirov, and A. Sobiczewski, Phys. Rev. C **86**, 064607 (2012).
[31] R. K. Choudhury and Y. K. Gupta, Phys. Lett. B **731**, 168 (2014).
[32] X. J. Bao, Y. Gao, J. Q. Li, and H. F. Zhang, Phys. Rev. C **91**, 011603(R) (2015).
[33] R. du Rietz, E. Williams, D. J. Hinde *et al.*, Phys. Rev. C **88**, 054618 (2013).
[34] G. G. Adamian, N. V. Antonenko, and W. Scheid, Phys. Rev. C **69**, 011601 (2004); **69**, 014607 (2004); **69**, 044601 (2004).
[35] Z.-H. Liu and J.-D. Bao, Phys. Rev. C **76**, 034604 (2007).
[36] Z.-H. Liu and J.-D. Bao, Phys. Rev. C **80**, 054608 (2009).
[37] V. I. Zagrebaev, A. V. Karpov, and W. Greiner, Phys. Rev. C **85**, 014608 (2012).
[38] T. Cap, K. Siwek-Wilczynska, M. Kowal, and J. Wilczynski, Phys. Rev. C **88**, 037603 (2013).
[39] N. Wang, E. G. Zhao, and W. Scheid, Phys. Rev. C **89**, 037601 (2014).
[40] W. Li, N. Wang, F. Jia, H. Xu, W. Zuo, Q. Li, E. Zhao, J. Li, and W. Scheid, J. Phys. G: Nucl. Phys. **32**, 1143 (2006).
[41] N. Antonenko, E. Cherepanov, A. Nasirov, V. Permjakov, and V. Volkov, Phys. Lett. B **319**, 425 (1993).
[42] N. V. Antonenko, E. A. Cherepanov, A. K. Nasirov, V. P. Permjakov, and V. V. Volkov, Phys. Rev. C **51**, 2635 (1995).
[43] A. S. Zubov, G. G. Adamian, N. V. Antonenko, S. P. Ivanova, and W. Scheid, Phys. Rev. C **65**, 024308 (2002).
[44] Z. Q. Feng, G. M. Jin, and J. Q. Li, Phys. Rev. C **80**, 057601 (2009).
[45] M. H. Huang *et al.*, Chin. Phys. Lett. **25**, 1243 (2008).
[46] G. Wolschin and W. Nörenberg, Z. Phys. A **284**, 209 (1978).
[47] J. Q. Li and G. Wolschin, Phys. Rev. C **27**, 590 (1983).
[48] P. Grangé, J. Q. Li, and H. A. Weidenmüller, Phys. Rev. C **27**, 2063 (1983).
[49] G. G. Adamian, N. V. Antonenko, and W. Scheid, Phys. Rev. C **68**, 034601 (2003).
[50] C. Y. Wong, Phys. Rev. Lett. **31**, 766 (1973).
[51] G. G. Adamian, N. V. Antonenko, R. V. Jolos, S. P. Ivanova, and O. I. Melnikova, Int. J. Mod. Phys. E **5**, 191 (1996).
[52] Y. T. Oganessian *et al.*, Phys. Rev. C **70**, 064609 (2004).
[53] Y. T. Oganessian *et al.*, Phys. Rev. C **76**, 011601(R) (2007).
[54] Y. T. Oganessian *et al.*, Phys. Rev. C **69**, 054607 (2004).
[55] Y. T. Oganessian *et al.*, Phys. Rev. C **87**, 014302 (2013).
[56] Y. T. Oganessian *et al.*, Phys. Rev. C **74**, 044602 (2006).
[57] Y. T. Oganessian *et al.*, Phys. Rev. C **87**, 054621 (2013).
[58] V. I. Zagrebaev, M. G. Itkis, and Yu. Ts. Oganessian, Phys. At. Nucl. **66**, 1033 (2003).
[59] V. I. Zagrebaev, Nucl. Phys. A **734**, 164 (2004).
[60] V. Zagrebaev and W. Greiner, J. Phys. G **31**, 825 (2005).
[61] V. Zagrebaev and W. Greiner, J. Phys. G **34**, 1 (2007).
[62] V. I. Zagrebaev and W. Greiner, Nucl. Phys. A (2015), doi:10.1016/j.nuclphysa.2015.02.010.
[63] I. Muntian, Z. Patyk, and A. Sobiczewski, Phys. At. Nucl. **66**, 1015 (2003).
[64] M. Kowal, P. Jachimowicz, and A. Sobiczewski, Phys. Rev. C **82**, 014303 (2010).